

필름 블로잉 공정에서의 다중해

이주성, 정현욱, 현재천
고려대학교 화공생명공학과, 유변공정연구센터

Multiplicities in the Film Blowing Process

Joong Sung Lee, Hyun Wook Jung, Jae Chun Hyun
Department of Chemical and Biological Engineering,
Applied Rheology Center, Korea University

Introduction

The tubular film blowing process (Fig. 1), which is typically an extensional deformation process, produces biaxially-oriented thin film or sheet by simultaneously stretching polymer melts in the axial and radial directions. The film blowing is somewhat similar to fiber spinning and film casting in that all these are mainly governed by extensional flow with free surfaces. However, the major difference of the film blowing process compared with other processes is that two-directional deformation simultaneously occurs in the flow regime, allowing for the precise control of films with good physical and mechanical properties. Therefore, there have been many theoretical attempts and experimental observations on this process in last three decades due to its academic and industrial importance (Pearson and Petrie, 1970; Han and Park, 1975; Kanai and White, 1984; Cain and Denn, 1988; Cao and Campbell, 1992; Ghaneh-Fard *et al.*, 1996; Yoon and Park, 1999). So far, however, theoretical approaches on this instability have been limited to the isothermal case with fixed freezeline employing Newtonian or simple viscoelastic models like upper-convected Maxwell (UCM) based on the linear stability method, not showing any nonlinear characteristics of this process.

In the film blowing process, multiple solutions with more than one flow profile under the specific operating parameter set were observed. The existence of multiple steady state solutions in the film blowing process was found by Cain and Denn (1988) for isothermal case employing simple Newtonian and UCM fluids. In this study, multiplicities of steady flows, depending on operating conditions, have been scrutinized using nonisothermal modeling with Phan-Thien Tanner (PTT) fluids as a reasonable viscoelastic constitutive equation for extensional flow. By adopting more realistic governing equations, another multiple solutions are discovered in the higher blow-up ratio region, and unrealistic points such as showing infinite tension disappeared. The theoretical results are quantitatively confirmed by comparing with experiments.

Formulation of the Problem

Dimensionless governing equations of the nonisothermal film blowing with PTT fluids, based on the Pearson and Petrie (1970) are as follows.

Equation of continuity:

$$\frac{\partial}{\partial t} \left(rw \sqrt{1 + \left(\frac{\partial r}{\partial z} \right)^2} \right) + \frac{\partial}{\partial z} (rwv) = 0 \quad (1)$$

Equation of motion:

Axial force balance:

$$\frac{2rw\sigma_{11}}{\sqrt{1 + \left(\frac{\partial r}{\partial z} \right)^2}} + B(r_F^2 - r^2) = T_z \quad (2)$$

Circumferential force balance:

$$B = w \left(\frac{-\sigma_{11}(\partial^2 r / \partial z^2)}{\sqrt{1 + \left(\frac{\partial r}{\partial z} \right)^2}^3} + \frac{\sigma_{33}}{r \sqrt{1 + \left(\frac{\partial r}{\partial z} \right)^2}} \right) \quad (3)$$

Constitutive equation (PTT model):

$$K\tau + De \left[\frac{\partial \tau}{\partial t} + \nabla \cdot \underline{v} - \underline{L} \cdot \tau - \tau \cdot \underline{L}^T \right] = 2D \quad (4)$$

where, $K = \exp(\epsilon De \text{tr } \tau)$, $\underline{L} = \nabla v - \xi D$, $2D = [\nabla v + \nabla v^T]$

Equation of energy:

$$\frac{\partial \theta}{\partial t} + \frac{v}{\sqrt{1 + \left(\frac{\partial r}{\partial z} \right)^2}} \frac{\partial \theta}{\partial z} + \frac{h}{w} (\theta - \theta_c) + \frac{E}{w} (\theta^4 - \theta_\infty^4) = 0 \quad (5)$$

Boundary conditions:

$$r = r_0 = 1, w = w_0 = 1, v = v_0 = 1, \tau = \tau_0, \theta = \theta_0 = 1 \quad \text{at } z=0$$

$$\frac{\partial r}{\partial t} + \frac{\partial r}{\partial z} \frac{v}{\sqrt{1 + (\partial r / \partial z)^2}} = 0, \frac{v}{\sqrt{1 + (\partial r / \partial z)^2}} = D_R, \theta = \theta_F \quad \text{at } z=x_F$$

where, r denotes dimensionless bubble radius, w dimensionless film thickness, v dimensionless velocity, t dimensionless elapsed time, z dimensionless spatial coordinate in flow direction, B dimensionless blow-up pressure, T_z dimensionless axial tension, θ dimensionless bubble temperature, τ dimensionless extra stress tensor, σ dimensionless total stress tensor, h dimensionless heat transfer coefficient, D_R drawdown ratio, and x_F freezeline height. The boundary condition at the freezeline height denotes no deformation over this position.

Several assumptions have been incorporated. First, the thin film approximation that all state variables only depend on one spatial coordinate, z , simplifies this system to a one-dimensional model. Second, the bubble shape is axisymmetric. Third, secondary forces acting on the bubble such as inertia, gravity, air-drag, and surface tension are neglected. Fourth, crystallization kinetics of polymer liquids is not considered here. Finally, the origin of the flow distance is chosen at the point of extrudate (die) swell, meaning that all pre-history deformations of polymer melts inside the die is not included in the present model.

Results

Figure 2 shows isothermal steady solutions on the TR-BUR plane of (a) UCM fluids and (b) PTT fluid under the given material conditions at a fixed freezeline height, $x_f=5$, when dimensionless bubble pressure (B) and dimensionless axial tension (T_z) are varied. In the Fig. 2(a), all points ultimately go to BUR=1 and TR=50, albeit tension is enormously increased. These behaviors of UCM fluid reveal that there is a limitation to describe extension deformation flow due to characteristic of UCM model, which shows divergence of the stresses at an extension rate. Whereas, PTT model in Fig. 2(b) does not show these unrealistic phenomena. That is, the film thickness is continuously decreased without any concentration point, as the axial tension goes up.

Figure 3 shows the multiplicity of the nonisothermal steady state solutions on the TR-BUR map. In this case, another multiple solutions were found in the higher blow-up ratio region. To compare with experimental data, these three points on the TR-BUR map having same bubble pressure and draw ratio, not axial tension like the isothermal case. Differ from isothermal case, which is fixed freezeline height, the freezeline height of nonisothermal model is calculated by the glass transition of the sample. For the isothermal case, the bubble pressure is continuously decreased as the BUR increased. That is, the bubble pressure shape shows like quadratic function of the BUR. Whereas, for the nonisothermal model, shows like cubic function, consequently, bubble pressure decreasing region only exist up to BUR=3. In the experimental studies, same behavior of the bubble pressure was observed.

Acknowledgements

This study was supported by research grants from the Korea Science and Engineering Foundation (KOSEF) through the Applied Rheology Center (ARC), and official KOSEF-created engineering research center (ERC) at Korea University, Seoul, Korea.

References

- Pearson, J. R. A., and C. J. S. Petrie, 1970, The Flow of a Tubular Film. Part I. Formal Mathematical Representation, *J. Non-Newtonian Fluid Mech.*, **40**, 1.
- Han, C. D., and J. Y. Park, 1975, Studies on Blown Film Extrusion. II. analysis of the Deformation and Heat Transfer Processes, *J. Appl. Polym. Sci.*, **19**, 3277.
- Kanai, T., and J. L. White, 1984, Kinematics, Dynamics and Stability of the Tubular Film Extrusion of Various Polyethylenes, *Polym. Eng. Sci.*, **24**, 1185.
- Cain, J. J., and M. M. Denn, 1988, Multiplicities and Instabilities in Film Blowing, *Polym. Eng. Sci.*, **28**, 1527.
- Cao, B., and G. A. Campbell, 1992, Aerodynamics in the Blown Film Process, *Polym. Eng. Sci.*, **32**, 751.
- Ghaneh-Fard, A., P. J. Carreau, and P. G. Lafleur, 1996, Study of Instabilities in Film Blowing, *AIChE J.*, **42**, 1388.
- Yoon, K.-S., and C.-W. Park, 1999, Stability of a Blown Film Extrusion Process, *Int. Polym. Proc.*, **14**, 342.

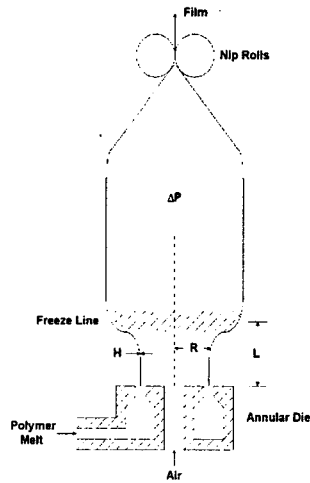


Figure 1. Schematic diagram of the film blowing process

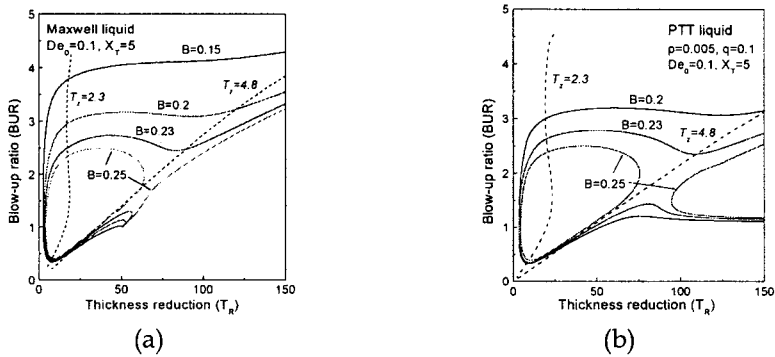


Figure 2. Isothermal steady state solutions of (a) UCM fluids and (b) PTT fluids

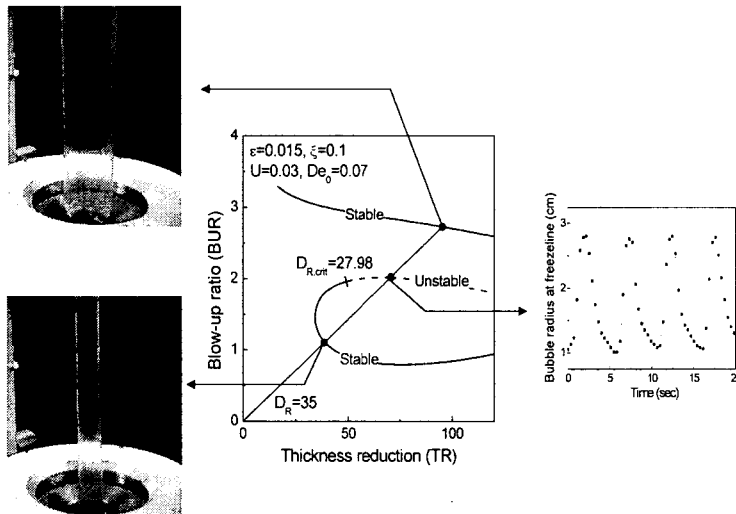


Figure 3. Nonisothermal steady state solutions with experimental data